Missing Optomotor Head-Turning Reflex in the DBA/2J Mouse

Peter Barabas,[1] *Wei Huang,*[1] *Hui Chen,*[1] *Christopher L. Koehler,*[2] *Gareth Howell,*[3] *Simon W. M. John,*[3] *Ning Tian,*[1] *René C. Rentería,*[2] *and David Križaj*[1,4]

Purpose. The optomotor reflex of DBA/2J (D2), DBA/2J-*Gpnmb*$^{+}$ (D2-*Gpnmb*$^{+}$), and C57BL/6J (B6) mouse strains was assayed, and the retinal ganglion cell (RGC) firing patterns, direction selectivity, vestibulomotor function and central vision was compared between the D2 and B6 mouse lines.

Methods. Intraocular pressure (IOP) measurements, real-time PCR, and immunohistochemical analysis were used to assess the time course of glaucomatous changes in D2 retinas. Behavioral analyses of optomotor head-turning reflex, visible platform Morris water maze and Rotarod measurements were conducted to test vision and vestibulomotor function. Electroretinogram (ERG) measurements were used to assay outer retinal function. The multielectrode array (MEA) technique was used to characterize RGC spiking and direction selectivity in D2 and B6 retinas.

Results. Progressive increase in IOP and loss of Brn3a signals in D2 animals were consistent with glaucoma progression starting after 6 months of age. D2 mice showed no response to visual stimulation that evoked robust optomotor responses in B6 mice at any age after eye opening. Spatial frequency threshold was also not measurable in the D2-*Gpnmb*$^{+}$ strain control. ERG a- and b-waves, central vision, vestibulomotor function, the spiking properties of ON, OFF, ON-OFF, and direction-selective RGCs were normal in young D2 mice.

Conclusions. The D2 strain is characterized by a lack of optomotor reflex before IOP elevation and RGC degeneration are observed. This behavioral deficit is D2 strain–specific, but is independent of retinal function and glaucoma. Caution is advised when using the optomotor reflex to follow glaucoma progression in D2 mice. (*Invest Ophthalmol Vis Sci.* 2011;52:6766–6773) DOI:10.1167/iovs.10-7147

From the Departments of [1]Ophthalmology and Visual Sciences and [4]Physiology, Moran Eye Center, University of Utah, Salt Lake City, Utah; the [2]Department of Physiology and Center for Biomedical Neuroscience, University of Texas Health Science Center at San Antonio, San Antonio, Texas; and [3]The Jackson Laboratory, Howard Hughes Medical Institute, Bar Harbor, Maine.

Supported by The International Retina Research Foundation (PB); National Eye Institute Grants EY13870 (DK), EY012345 (NT), and P30EY014800 (NT, DK); The Foundation Fighting Blindness (DK), the Moran TIGER Award (DK), and an unrestricted grant from Research to Prevent Blindness to the Moran Eye Institute and Dept. of Ophthalmology at the University of Utah. SWMJ is a Howard Hughes Medical Institute investigator.

Submitted for publication December 27, 2010; revised April 20 and June 2, 2011; accepted June 27, 2011.

Disclosure: **P. Barabas**, None; **W. Huang**, None; **H. Chen**, None; **C.L. Koehler**, None; **G. Howell**, None; **S.W.M. John**, None; **N. Tian**, None; **R. C. Rentería,** None; **D. Križaj**, None

Corresponding author: Peter Barabas, John Moran Eye Center, Room S4140, University of Utah School of Medicine, 65 N. Mario Capecchi Drive, Salt Lake City, UT 84132; sirmook12@gmail.com.

The DBA/2J (D2) strain has become an important animal model of pigmentary glaucoma.[1–8] The D2 strain carries recessive alleles in genes coding for *Gpnmb* (*Gpnmb*^{R150X}) and *Tyrp1* (*Tyrp1*^{b}). The two mutations are both necessary and sufficient to induce iris pigment dispersion (*ipd*) and iris stromal atrophy (*isa*) phenotypes in D2[3,9,10] and C57BL/6J (B6)[11] strains. In the anterior chamber of 6- to 8-month-old D2 eyes, dispersed pigment disrupts aqueous outflow drainage and elevates intraocular pressure (IOP).[3,12] The sustained increase in IOP has been correlated with optic neuropathy, retinal ganglion cell (RGC) loss, and, ultimately, optic disc cupping in D2 animals older than ~9 months.[3] Because the phenotype observed in D2 mice resembles pathophysiological changes occurring in patients with glaucoma,[13] the D2 strain is now one of the most widely used animal models of glaucoma.[3,4,12]

The noninvasive analysis of spatial frequency threshold (also termed spatial visual acuity) developed by Prusky et al.[14,15] is an efficient, reproducible, and widely used method of assessing the functional state of rodent vision.[16–23] The optomotor paradigm tests the rodent spatial frequency threshold by measuring reflexive orienting responses to vertical gratings, drifting horizontally across the visual field at different spatial frequencies. We intended to use the method to track the progress of glaucomatous degeneration in D2 animals from eye opening to 14 months of age. Surprisingly, no optomotor head-tracking responses were detected, even in the youngest animals, suggesting that visual acuity in the D2 strain is compromised significantly earlier than increases in IOP and axonal degeneration are observed.[1,10,12] Since the tracking response requires full visual and motor functionality, we assessed neuronal signals in the outer and inner retina and conducted behavioral tests of motor and vestibular function and visual tasks to pinpoint the locus of deficiency. The D2 strain exhibited a nonretinal, nonvestibular, central vision-independent deficit that is independent of mutations in *Tyrp1* and *Gpnmb* genes. Hence, caution is advised when behavioral analyses of visual function are performed using this popular and ubiquitous glaucoma model.

Methods

Animals

All procedures were approved by Institutional Animal Care and Use Committee (IACUC) at the University of Utah, University of Texas, and The Jackson Laboratory, according to the guidelines established by the ARVO Statement for the Use of Animals in Ophthalmic and Vision Research. C57BL/6J (B6) and DBA/2J (D2) mice were from The Jackson Laboratory (Bar Harbor, ME). This study analyzed separate D2 colonies maintained at four locations: the Križaj and Vetter laboratories at the University of Utah, the Rentería laboratory at the University of Texas Health Science Center at San Antonio, and the John laboratory at The Jackson Laboratory. To assess potential roles of glaucoma-relevant genes and phenotypes in the loss of optomotor response, we included

two control strains: (1) D2-*Gpnmb*$^{+}$, which is genetically identical with D2 except for a wild–type version of *Gpnmb*. This strain does not develop the prominent iris pigment dispersion phenotype, high IOP or glaucoma in our colony. D2-*Gpnmb*$^{+}$ mice do develop the iris stromal atrophy phenotype, which is caused by the *Tyrp1*^{b} mutation expressed in D2 mice.[10] (2) The B6.*isa*^{D2}*ipd*^{D2} strain (also known as B6.*Gpnmb*^{R150X}*Tyrp1*^{b}) is a B6 congenic strain that is homozygous for the *isa* and *ipd* congenic intervals derived from D2. These animals carry both the *Gpnmb*^{R150X} and the *Tyrp1*^{b} mutations and develop a disease of the iris that is indistinguishable from D2 mice, yet rarely develop high IOP or glaucoma.[11] The extent of the D2-derived *isa* and *ipd* regions are approximately 23.6 to 63.2 Mb (chromosome 6, *ipd*) and 10.0 to 36.8 Mb (chromosome 4, *isa*), respectively.[11]

Behavioral Tests

Optomotor reflex-based spatial frequency threshold tests were conducted in a visuomotor behavior measuring system (OptoMotry; CerebralMechanics, Lethbridge, AB, Canada) that displays a virtual rotating cylinder with a vertical black-and-white sinusoidal grating pattern in photopic conditions (illuminance inside the box was approximately 165 lux) to light-adapted mice. Mice aged between eye opening and 14 months (see Supplementary Table S1, http://www.iovs.org/lookup/suppl/doi:10.1167/iovs.10-7147/-/DCSupplemental, for a breakdown by strains, age categories, and sex) were placed on a 2-in diameter pedestal in a box with 4 LCD displays on each side. The center of the virtual rotating cylinder was maintained at the position of the mouse head. The experimenter observed the behavior of the mouse during presentation of the rotating stimuli and indicated to the software whether a tracking movement of the head was elicited. Tracking was defined as a reproducible smooth pursuit with a velocity and direction concordant with the stimulus. Trials of each direction and spatial frequency were repeated until the presence or absence of the tracking response could be established unequivocally. Spatial frequency of the stimulus was stepped up or down with the staircase method[23] to find the behavioral threshold, corresponding to the visual acuity for the behavior. Rotation speed (12°/s) and contrast (100%) were kept constant unless no response was found at any of the tested spatial frequencies. Measurements were conducted blind to the genotype of the mice.

The Rotarod test was conducted to measure the time a mouse is able to stay on a rotating rod. Rotor speed was gradually increased from 0 to 6 rpm in 1 minute and maintained at that speed for 5 more minutes. All mice (three per group, aged 1 month) were tested three times.

The visible platform test was conducted in a Morris water maze tank, four feet in diameter, filled with clear water at room temperature (~25°C), with a white platform rising above the water line. The platform was lined with a black stripe at the water line. Each animal (4 B6 and 6 D2 mice, all aged 1 month) was allowed a maximum of 60 seconds per trial to mount the platform and was started at four different locations with a 20-second interval on a warming pad between starts. The time to reach the visible platform from each starting location was measured for each mouse once per day for 2 days, and the mean for each group was compared using the Mann-Whitney statistical test.

Phenotyping

Gene expression profiling of whole isolated retinas was done using total RNA extracted (Trizol; Invitrogen, Carlsbad, CA) and converted to cDNA (SuperScript III First-Strand Synthesis kit; Invitrogen). Amplification of PCR products with a thermocycler (Veriti; Applied Biosystems, Inc., [ABI], Foster City, CA) was measured by fluorescence, through binding of double-stranded cDNA to SYBR Green (ABI) in the reaction mixture. After amplification, the ratio of the Brn3a mRNA to the glyceraldehyde-3-phosphate dehydrogenase (*Gapdh*) reference gene was calculated for each sample. Twelve to 15 independent samples (retinas) were used for each age group. Transcript level in a random control animal sample was chosen as 1, and all other samples were normalized to that sample.

Intraocular pressure (IOP) measurements of Avertin-anesthetized (250–300 mg/kg body weight) mice were conducted with a handheld tonometer (TonoLab; Tiolat Oy, Helsinki, Finland) system. Body temperature was kept stable with the help of an isothermal pad heated to 37°C (Braintree Scientific Inc, Braintree, MA). Care was taken to keep the head of the mice level, as head position can exert a considerable influence on the IOP measurement.[24]

Immunohistochemical analysis of frozen retinal sections was conducted as described elsewhere.[25,26] Briefly, mice were anesthetized and euthanatized with isoflurane (Minrad, Inc., Bethlehem, PA), followed by cervical dislocation. Eye cups were fixed in 4% (wt/vol%) paraformaldehyde in phosphate-buffered solution (PB, 0.1 M; pH 7.4), cryoprotected in ice-cold 30% sucrose, embedded in OCT (Tissue-Tek; VWR, Scientific Inc., Media, PA) and cut into 16-μm slices. Sections were washed in PB for 15 minutes, then permeabilized and blocked with 0.5% Triton X-100 and 10% goat serum. The Brn3a (Chemicon International, Temecula, CA) mouse antibody was used at 1:100 (overnight, 4°C), and detected with Alexa Fluor 488 nm goat anti-mouse secondary antibody (Invitrogen), diluted at 1:1000 (room temperature, 3 hours). Sections covered with aqueous mounting medium (FluoromountG; Southern Biotech, Birmingham, AL) were examined by confocal microscopy (LSM 510; Carl Zeiss Meditec, Inc.). Settings and image-acquisition parameters were identical for D2 and D2-*Gpnmb*$^{+}$ sections.

Assays of Retinal Function

Electroretinography (ERG) was performed on D2 mice (1.5 months old; $n = 3$) and B6 mice (3 months old; $n = 3$) kept in darkness overnight. The mice were anesthetized in dim red light with ketamine/xylazine (90 mg/10 mg per kg body weight) and placed on a chemical hand warmer that maintained temperature at 37°C to 38°C for the duration of the experiment. The pupil was dilated with 1% tropicamide, and ERGs were measured (UTAS E-3000; LKC Technologies, Gaithersburg, MD) between a gold corneal and a stainless-steel scalp electrode with a 0.3- to 500-Hz band-pass filter. Scotopic, followed by photopic (135 lux background) ERGs were recorded with flash intensities increasing from 0.0025 to 250 cd · s/m^2 and 0.25 and 250 cd · s/m^2 respectively. The photoflash unit was calibrated by LKC Technologies to deliver 2.5 cd · s/m^2 at 0 dB flash intensity. Flash intensity was calculated according to the formula: dB = 10 log (I/I_o); where I_o is flash intensity at 0 dB, and I is the actual flash intensity. The a- and b-wave amplitudes and latencies were determined in scotopic and photopic conditions, and the mean values at each stimulus intensity compared with an unpaired two-tailed *t*-test with Bonferroni correction for multiple comparisons.

Multielectrode array (MEA) recordings were performed essentially as described previously.[27] Briefly, 1.5-month-old, dark-adapted D2 mice ($n = 4$) were killed, their retinas isolated and placed RGC-side down in an MEA recording chamber (MEA-60; MultiChannel Systems, Reutlingen, Germany) kept at 30°C. Acquired voltage signals were band-pass filtered at 0.1 Hz to 3 kHz and sampled at 20 kHz (MCRack; MultiChannel Systems). Extracellular spiking responses to visual stimuli consisting of checkerboards of Gaussian white-noise at 75 Hz were presented using the Psychophysics Toolbox extensions to MatLab (The Mathworks, Natick, MA).[28–30] Spikes were sorted into individual RGC spike trains (Offline Sorter software; Plexon, Dallas, TX). The series of images that preceded every spike was averaged for each RGC, yielding a stimulus movie that represented a spatiotemporal map of the most effective stimulus for that RGC. Pixel values over the center of the receptive fields of RGCs were averaged and plotted for every frame in time to generate the linear filters, examples of which are shown in Figure 4. Receptive field diameter was defined as the average diameter at one SD of the 2D Gaussian fit of the frame having pixel intensities with the largest deviation from the mean.[27]

Directionally selective (DS) RGC analysis with MEAs was conducted in retinas of 1.5-month-old B6 ($n = 7$) and 1.5-month-old D2 ($n = 7$)

mice.[31] Retinas were isolated in infrared light and placed in an MEA-60 chamber. Action potentials evoked by a moving (1000 mm/s), white, rectangular bar (600 × 4000 μm) were recorded from retinal neurons located in the ganglion cell layer. The stimulus was tested using 12 directions at 30° intervals. Spike sorting as described above was used to assign spikes to spike trains representing the responses of individual neurons. The peak spike frequency of the leading and trailing edge (ON and OFF) responses were averaged from 50 responses for each cell. The directional selectivity index (DSI) was defined as:

$$\text{DSI} = (\text{preferred peak frequency} - \text{null peak frequency})/(\text{preferred peak frequency} + \text{null peak frequency})$$

Statistical Analysis

Data are presented as mean ± SEM (Instat statistical software; ver. 3.0b for Macintosh; GraphPad Software, San Diego, CA). After a normal distribution was confirmed, a parametric test was used at $P < 0.05$. One-way ANOVA with Bonferroni post hoc test was used to compare multiple groups or a two-tailed unpaired Student's *t*-test with Welch correction (for unequal variations) to compare two groups of data, unless specifically noted otherwise.

Results

The D2 Strain Does Not Respond to Optokinetic Stimulation

D2 mice aged from 14 days to 1, 4, 8, 11, and 14 months were stimulated with drifting gratings at 100% contrast. None of the D2 animals at any age were able to track the stimuli at any drift speed (1–30 deg/s) or spatial frequency (0.03–0.5 cyc/deg; $n = 28$; Fig. 1). Weak fleeting responses that could not be reproduced were noted occasionally; however, these were not bona fide tracking movements (see the Methods section and Supplementary Movie S1 for a typical B6 response and Supplementary Movies S2 and S3 for typical and atypical D2 behavior, http://www.iovs.org/lookup/suppl/doi:10.1167/iovs.10-7147/-/DCSupplemental). To determine whether this phenotype was strain specific or caused by the specific mutations in *Gpnmb*, experiments were repeated in D2-*Gpnmb*$^{+}$ mice, which do not develop high IOP or glaucomatous optic neuropathy.[10] Surprisingly, these mice ($n = 8$) also lacked optomotor head-tracking responses, indicating that the D2 phenotype is not affected by Gpnmb loss of function. To rule out effects of both *Gpnmb*^{R150X} and *Tyrp1*^{b} mutations, optomotor responses were assessed in B6.*isa*^{D2}*ipd*^{D2} mice (see the Methods section). Despite being homozygous for mutations in both genes, these mice had a measurable spatial frequency threshold that was decreased by 17% at 5 months of age compared with age-matched B6 acuity. A small but significant difference ($P < 0.001$) was observed between B6.*isa*^{D2}*ipd*^{D2} males (0.354 ± 0.007, $n = 3$) and females (0.264 ± 0.004, $n = 3$). No other differences between the sexes were observed for any of the other strains, and although a difference between the sexes for this strain cannot be ruled out, it is probably due to chance. Further analysis of potential sex-related differences may need to be performed on this strain. In addition, photopic spatial frequency thresholds in the first generation from D2 and B6 crosses were significantly higher ($P < 0.001$) than in B6 mice, suggesting that recessive D2 alleles underlie the lack of head-tracking behavior in D2 mice. Overall, these results demonstrate that the presence of optomotor reflex in D2 and B6 mouse lines is a strain-specific trait that is not related to the known glaucoma-causing mutations.

Aged but Not 1- to 3-Month-Old D2 Mice Exhibit Signs of Glaucoma

We checked for two of the major hallmarks of glaucoma progression (Fig. 2): IOP increase and RGC markers. Our previous investigations showed that a high proportion of D2 retinas older than 12 months exhibit signs of neurodegeneration typical of RGC neuropathy, including decreased mRNA expression of the RGC markers Brn3a and VGLUT2 and loss of RGC somata and axons, whereas few changes in mRNA or protein levels were observed before the IOP increase at >6 months.[1,3,10,25] As reported previously[1,10,25] IOP levels increased significantly above 20 mm Hg at 9 months ($P = 0.015$; Fig. 2A) and Brn3a immunoreactivity in D2-*Gpnmb*$^{+}$ retinal sections was indistinguishable from B6 controls.[10,12] These

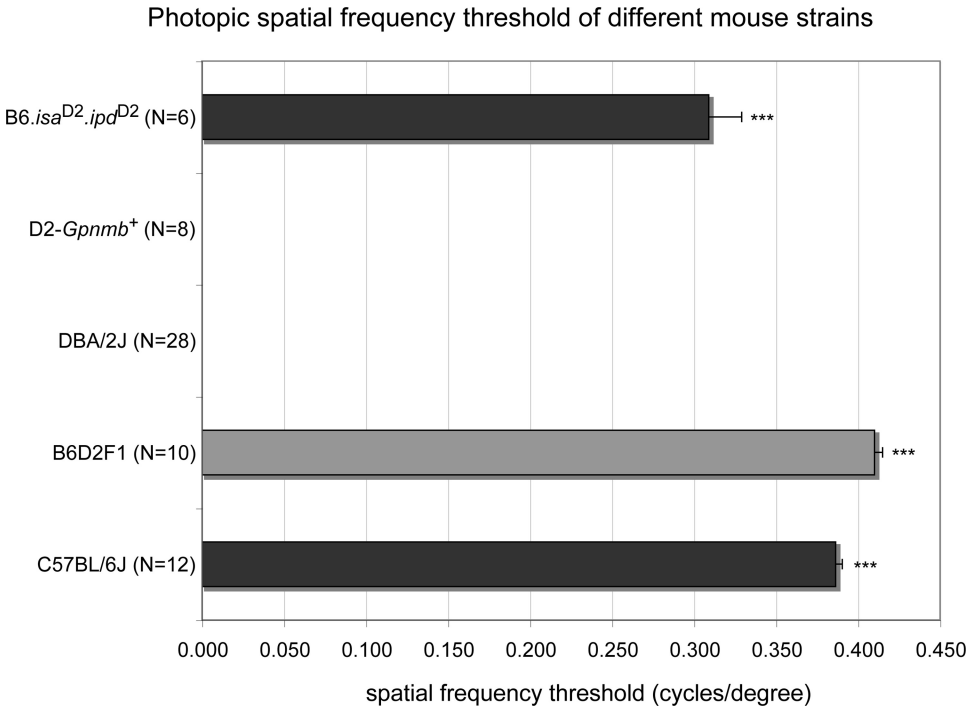

Figure 1. Photopic spatial frequency threshold estimated through the optomotor reflex in mouse strains, based on B6 and D2 genetic backgrounds. D2-*Gpnmb*$^{+}$ and D2 mice, never elicited a response; thus, acuity was 0. The B6-based B6.*isa*^{D2}*ipd*^{D2} strain carried the D2 versions of *isa* and *ipd* regions. B6D2F1 mice are the first generation of a B6 and D2 cross. *n*, the number of older than 1 month old mice tested, $^{***}P < 0.001$.

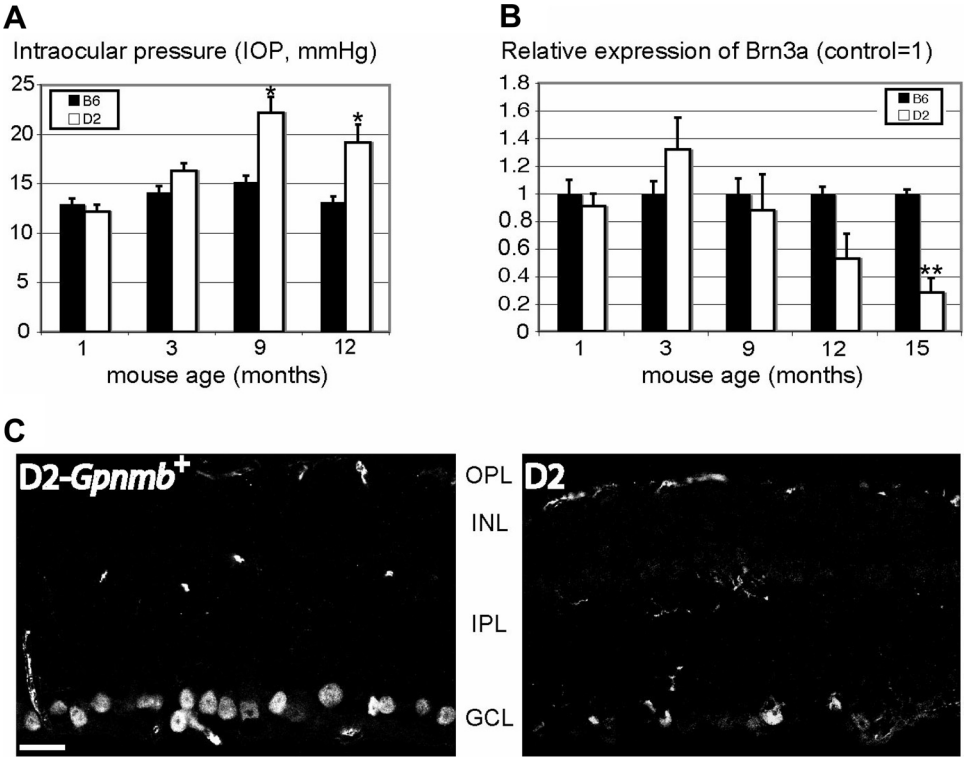

FIGURE 2. Increased IOP (**A**) and decreased expression of the RGC marker Brn3a (**B**, **C**) in DBA/2J retinas were apparent after 9 and 12 months, respectively. Immunofluorescent images (**C**) of retinal slices showed a marked difference in Brn3a antibody labeling of D2-*Gpnmb*$^{+}$ (control) and D2 mice. Twelve-month-old D2 mice diagnosed with severe glaucoma showed extensive loss of Brn3a-positive RGCs compared with control mice of the same age. $^{*}P < 0.05$; $^{**}P < 0.01$. Scale bar, 20 μm.

qualitative data demonstrate that the lack of optomotor reflex in D2 mice was not caused by genotype-specific loss of RGCs.

No Defects in ERG, Major RGC Functional Classes, or DS Cells

We sought to determine whether the D2 phenotype is caused by compromised visual signaling in the retina. ERGs (i.e., corneal field potentials in response to light stimuli) were recorded in B6 and D2 animals. Neither scotopic nor photopic ERG a-wave (not shown) and b-wave amplitudes (Fig. 3B) and implicit times were significantly different in D2 mice compared with B6 mice. ERGs (Fig. 3A) show a somewhat different wave shape because these are different strains, but the measured variables (amplitude, latency) all suggest normal function of the outer retina of D2 animals.

Next, light-evoked responses of RGCs were measured directly in intact retinas using MEA recording. Retinas from D2 mice exhibited typical RGC light responses without obvious deficits (Fig. 4). RGC responses measured in D2 animals are comparable to spiking patterns previously recorded from B6 retinas.[32] Spike-triggered averaging of the checkerboard image sequences (i.e., the images preceding every spike) was used to generate linear filters that represent the most effective intensity time course of receptive field center illumination for stimulating the RGCs.[32] This approach has also been used to sort RGCs into functional classes.[32] Linear filters from D2 RGC responses fit with a difference of Gaussian function had time courses and shapes similar to that reported for B6 RGCs (Fig. 4A).[32] We did not find significant deficits, either in the histograms of RGC receptive field

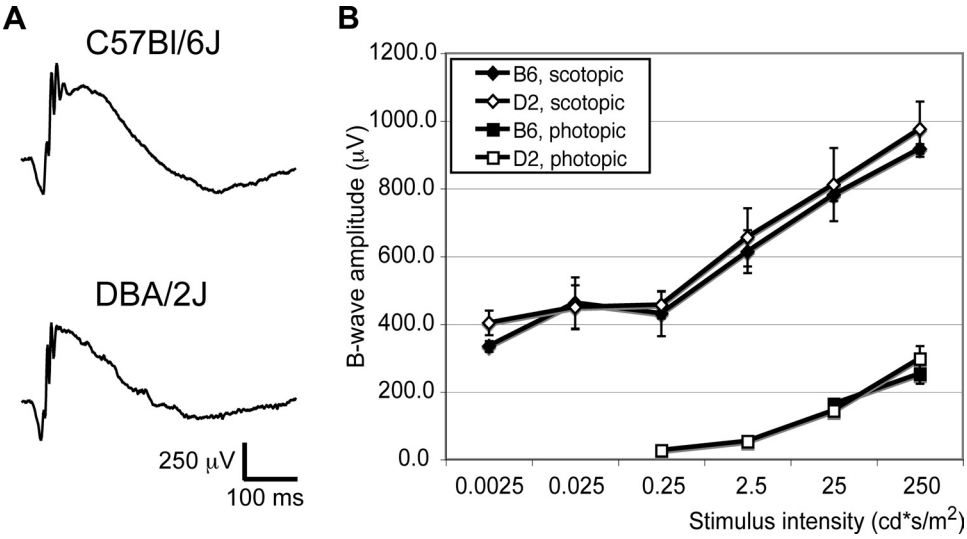

FIGURE 3. Representative scotopic ERG sample (raw data) traces (**A**) evoked by a 25 cd · s/m^2 flash and analysis (**B**) of b-wave amplitudes in both scotopic and photopic conditions show no abnormalities in the ERG of D2 mice (1.5 months, $n = 3$) when compared to B6 mice (3 months, $n = 3$).

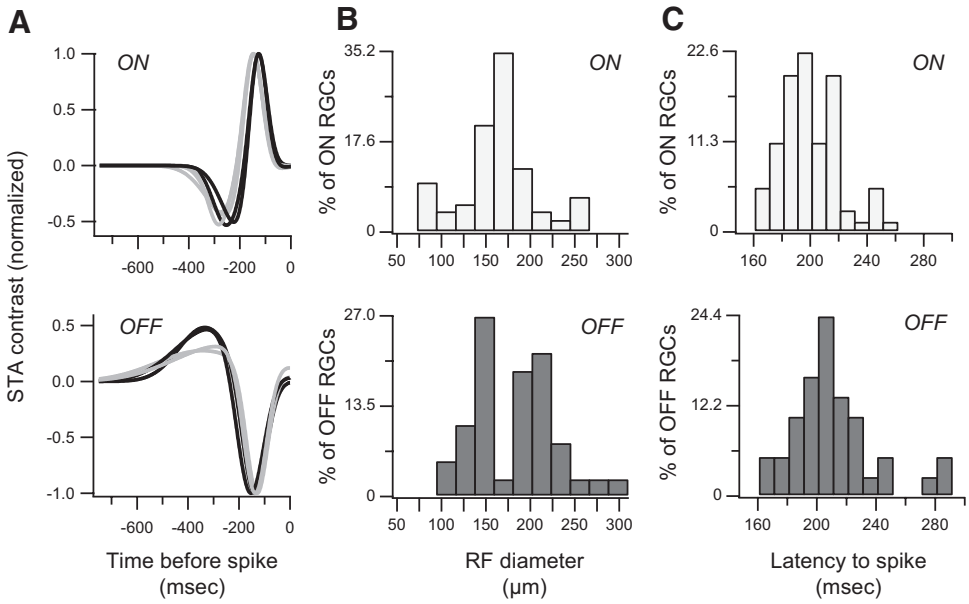

Figure 4. Retinas from D2 mice had typical RGC light responses without obvious deficits. (**A**) Linear filters constructed from RGC responses to white-noise checkerboard stimulation and fit with the Naka-Rushton function had normal time courses and shapes. five of seven ON RGCs (*top*) from a single retina showing medium (*gray*) and fast (*black*) types and four of 5 OFF RGCs (*bottom*) from the same retina showing monophasic (*gray*) and biphasic (*black*) types as described by Kerschensteiner et al.,[32] are shown. An RGC's linear filter represents the most effective intensity time course of receptive field center illumination for stimulating that RGC. (**B**) Histograms of receptive field center diameters of ON (*top*) and OFF (*bottom*) RGCs are shown. Bar heights are the fraction of total RGCs recorded (71 ON cells and 37 OFF cells from four retinas). (**C**) Histograms of latency to spiking based on linear filter major peak location of ON (*top*) and OFF (*bottom*) RGCs are shown. Bar heights represent the fraction of total RGCs recorded.

center diameters (Fig. 4B) or the histograms of latency to RGC spiking (Fig. 4C).

Optokinetic responses themselves are likely to be mediated by a type of wide-field direction-selective (DS) RGCs.[33,34] To compare the properties of DS RGCs in D2 and B6 mice, DS responses were characterized by recording RGC responses to a directional stimulus and calculating a direction-selective index (DSI). RGC firing responses to moving light bars revealed DS and non-DS cells in D2 retinas (Figs. 5A, 5B). D2 and B6 retinas did not differ significantly in the cumulative probability of finding an RGC with a particular DSI for ON ($P = 0.71$) and OFF ($P = 0.99$) RGCs. A small yet statistically significant ($P = 0.0005$) increase in the probability of eliciting a direction-selective OFF response was observed in D2 ON-OFF cells. However, no difference between D2 and B6 mice was observed with respect to the ON component's direction selectivity of the ON-OFF RGCs ($P > 0.9999$).

D2 Mice Have Functional Central Vision and Vestibulomotor Responses

Central vision of D2 mice that had undergone optomotor testing was subsequently investigated with a visible platform swim task. Experiments using the Morris water tank showed normal central vision in D2 mice. The average time needed for 1-month-old D2 animals to find the visible platform was 16.6 ± 5.5 seconds ($n = 6$), not different ($P = 0.68$) from the 16.3 ± 4.3 seconds ($n = 4$) measured in B6 animals. Thus, mice that completely lacked the optomotor reflex had functional central vision that allowed them to find the platform in a manner indistinguishable from B6 mice. Likewise, the Rotarod test showed no difference between D2, B6, and D2-*Gpnmb*$^{+}$ cohorts (age for all groups, 1 month). All tested animals were able to remain on the rotating rod at the highest tested speed for at least 6 minutes, indicating that vestibulomotor function in D2 animals is normal.

Discussion

Although the D2 strain represents one of the best-studied mouse glaucoma models in terms of IOP, neuronal, and glial changes,[1,6,12] functional analysis of glaucoma progression has been lacking a dedicated, fast, and noninvasive method. Development of a physiological test that would measure focal RGC loss in mice would be highly desirable for evaluating the progressive loss of visual function in models of chronic glaucoma. One promising method that has been increasingly used to evaluate mouse vision due to its convenience and reproducibility is the optomotor reflex–based measurement of spatial frequency threshold.[14] When studied with this technique, B6 mice provide spatial frequency threshold values (0.37–0.4 cyc/deg; see Refs. 14, 15, 22, 23 and this study) across different laboratories. Whereas the method is highly reproducible in wild-type mouse strains such as B6 and Sv129, analyses of optomotor behavior in D2 mice have tended to yield inconsistent results. In two recent studies, the mean photopic spatial frequency threshold of D2 mice has ranged from 0.33 cyc/deg[35,36] to 0.55 cyc/deg,[37] whereas another comparative study of multiple mouse strains[38] failed to detect optomotor responses in D2 animals. Our results are consistent with the observations from Puk et al.[38] We report here that D2 mice did not exhibit optomotor head-tracking responses to laterally drifting spatial gratings at any age tested, starting from eye opening. This deficit was observed by three independent observers in separate colonies of mice from four different laboratories in Utah, Texas, and Maine.

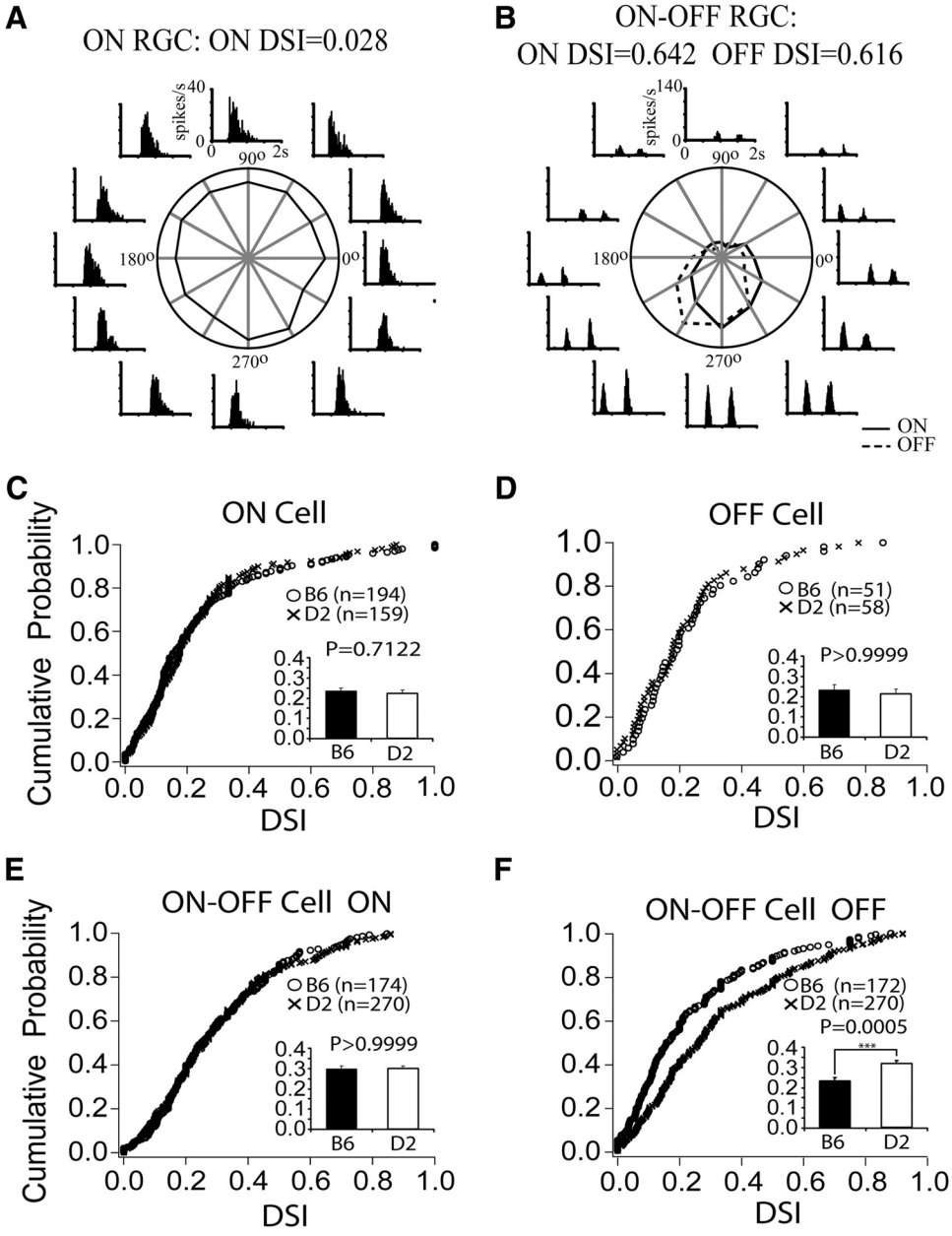

FIGURE 5. Representative example of a directionally nonselective (**A**) and a directionally selective (**B**) RGC. The cumulative probability of finding a RGC that was directionally selective was the same for both ON (**C**) and OFF (**D**) RGCs and for the ON response of ON-OFF cells (**E**) in B6 and D2 retinas. There was increased probability of directional selectivity in the OFF response of ON-OFF cells in the D2 retinas.

In a way, our results highlight a potential pitfall in this widely used technique for studying visual behavior in mice. In particular, it is imperative that the exact experimental protocols and criteria for accepting or not accepting head movements as tracking behavior are made available as they represent relevant information for adequate comparison of optomotor behavior in strains such as D2. Two potentially confounding factors need to be taken into account when interpreting results of optomotor measurements in the D2 strain. First, intense motor activity may both mask the optomotor tracking response and provide false-positive identifications to the experimenter. Such exploratory behavior in D2 mice does not subside in less than 30 minutes, is not disrupted by sudden visual (darkening/lighting up of displays) or acoustic stimuli, and has been referred to in the literature as "lack of attention" to visual stimuli.[36,38] Second, given that glaucomatous changes in the D2 retina reflect an ongoing iris disease, it is necessary to take into account optical aberrations that may reduce visual acuity in a progressive manner independent from glaucomatous changes. Hence, the appropriate control for D2 mice is the D2-*Gpnmb*$^{+}$ strain (developing iris stromal atrophy) used in this study, not the B6 strain. The B6 strain represents an appropriate control for the B6.*isa*^{D2}*ipd*^{D2} strain, both of which, in contrast to D2 animals, show normal optomotor behavior. This study is the first to employ D2-*Gpnmb*$^{+}$ and B6.*isa*^{D2}*ipd*^{D2} strains as controls for analysis of optomotor behavior in mice.

Results showing a lack of optomotor responses in DBA/2NCrl mice younger than 4 months were attributed to early degeneration of RGCs.[38] However, our data show that the optomotor deficit in D2 mice is independent of glaucomatous RGC death and optic nerve degeneration. Transcript levels of RGC markers Brn3a and VGLUT2[25] in <3 month-old D2 retinas were indistinguishable from levels in control eyes, whereas aged D2 mice showed pathologic changes consistent with the phenotype established and characterized in previous studies.[1,3,12] Likewise, IOP levels in D2 eyes were elevated after 6 months whereas significant loss of ganglion cells was observed only after the ninth month, consistent with previous re-

ports.[1,3,4,39] These results are in contrast with the study by Zhou et al.,[35] who reported an accelerated time course of degenerative changes in D2 retinas, pointing to a possible phenotypic divergence within the D2 strain. In light of the high variability of the D2 optomotor phenotype seen ranging from no reflex[38] to different spatial frequency threshold levels,[35–37] we speculate that the D2 strain may consist of substrains presenting different optomotor phenotypes. Importantly, the optomotor phenotype in D2 animals was identical to optomotor behavior of D2-*Gpnmb*$^{+}$ mice which carry a wild-type version of the *Gpnmb* gene and never develop the iris pigment dispersion phenotype, increased IOP, or RGC degeneration.[10] Hence, the observed lack of optomotor function in our D2 mice is a strain- not a disease-specific phenomenon. This conclusion was reinforced by measurements in B6 mice that carry glaucoma-promoting *Gpnmb*^{R150X} and *Tyrp*^{b} mutations,[11] yet exhibit robust optomotor reflexes. Hence, mutations that cause pigmentary glaucoma in mice do not in themselves eradicate the optomotor head-tracking response. In addition, lack of optomotor reflexes in young D2 mice cannot be attributed to optical changes that occur in the anterior part of the eye (due to iris stromal atrophy and iris pigment dispersion), because these pathologic changes do not take place until after 5 to 6 months in D2 mice.[10]

Tracking moving stimuli with head rotation represents a subset of the full optokinetic reflex, which encompasses both head- and eye movements. The two mechanisms act in parallel to ensure image stabilization on the mouse retina over a wide range of head and body motions.[40] An increase in the amplitude/rate of eye movement could reduce or eliminate the animal's need to move its head. However, this is unlikely, given that the eye-tracking response in D2 animals is characterized by half the number of tracking movements per minute compared with those in B6 mice.[41] Because eye and head-tracking systems are mediated by similar visual pathways,[15] it is also not likely that the deficit in head-tracking reflects dysfunctional retinal input to the accessory optic system.[34] Moreover, given that central visual performance of young D2 mice was comparable to other mouse strains (see Refs. 36, 42 and this study), we conclude that the animals are probably capable of retinal image stabilization.

What mechanism underlies the optomotor deficit in the D2 strain? Our data exclude most outer and inner retinal dysfunctions. Full-field flash ERGs and light-evoked firing of RGCs appeared normal in D2 animals, consistent with the observations that B6, D2, and D2-*Gpnmb*$^{+}$ strains show few statistically significant differences in ERG and PERG amplitude and latency.[43–45] No deficiency was observed in vestibulomotor function, consistent with the observation that motor coordination abilities of these mice are on par with those in B6 mice.[46] The average time needed to reach a visible platform was similar in young adults of D2 and B6 strains, suggesting that D2 mice have functional central vision.

The water-box behavioral analysis using visual stimulation based on black-and-white–striped patterns did not reveal visual deficiencies in D2 animals.[36,42] Since the water-box stimulus is stationary, whereas the optomotor stimulus is moving, this finding could indicate a possible selective deficit with respect to moving stimuli. Therefore, an obvious target for the D2 optomotor deficit was DS cells, wide-field RGCs that project to the dorsal, medial, and lateral terminal nuclei of the accessory optic system (AOS).[34,47,48] Surprisingly, analysis of DS responses in D2 animals revealed no difference in ON or OFF responsiveness but showed a slight increase in the cumulative probability of the OFF component in ON-OFF DS cells.

Although we cannot be 100% certain that an untested but potentially critical aspect of RGC function is deficient in D2 mice, we conclude that the functional deficit in the D2 optomotor reflex is likely to be downstream from the retina. Normal spontaneous RGC firing, DS RGC function, the optokinetic eye reflex, and the ability to see and swim to a visible platform in the D2 mouse exclude major deficits in the retinocollicular, retinogeniculate, geniculocortical, and retino-AOS pathways.

To establish the causal relationship between a specific gene and optomotor behavior, a sequential analysis of co-segregated traits in genetic crosses (F2, backcrosses, RI lines etc.) may have to be conducted in future studies. Such an approach would help identify polygenic contributions to a well-defined and easily observable behavior such as the optomotor reflex. Polygenic networks have a prominent role in brain function.[49] Accordingly, at least 77 genes and ESTs show >1.5-fold mean increase in brains of adult B6 compared with D2 mice,[50] with particular changes in genes that regulate signaling pathways, gene regulation, and metabolism whereas 41 genes showed higher expression in the brains of adult D2 mice versus B6 mice. The availability of phenotypically and genotypically characterized B6- and D2-derived strains provides a major advantage for using classic genetic approaches to characterize subtle shifts and genetic influences on behavioral traits. Considering the significant extent to which genomic sequences are conserved between humans and mice, such genetic-functional approaches may also have relevance for our understanding of genomic co-variance, polymorphisms, complex molecular cascades, and epigenetic regulation that appear to be increasingly important in determining complex behavioral phenotypes.

In summary, our data reveal a strain-specific behavioral phenotype in the D2 mouse strain that has been ubiquitously used as a model of chronic glaucoma. Our results demonstrate that the compromised optomotor reflex in D2 animals reflects a strain-specific trait (or combination of traits) rather than an early pathologic feature associated with glaucoma. The lack of the optomotor head-turning reflex in the D2 mouse strain can be observed well before the onset of any known pathologic changes. Although the optomotor head-tracking reflex is a useful method for following retinal disease progression, it is essential to use appropriate strain controls.

Acknowledgments

The authors thank H. Steve White (University of Utah) for the loan of the Rotarod system; Nikolai Akimov, David Medina, and Salvatore Oddo (University of Texas Health Science Center, San Antonio) for the help in data analysis and for conducting the visible platform swim tests; and Nazia M. Alam (Cornell University) for the training and advice with the visuomotor system setup (OptoMotry; CerebralMechanics).

References

1. John SW, Smith RS, Savinova OV, et al. Essential iris atrophy, pigment dispersion, and glaucoma in DBA/2J mice. *Invest Ophthalmol Vis Sci.* 1998;39:951–962.
2. Danias J, Lee KC, Zamora MF, et al. Quantitative analysis of retinal ganglion cell (RGC) loss in aging DBA/2NNia glaucomatous mice: comparison with RGC loss in aging C57/BL6 mice. *Invest Ophthalmol Vis Sci.* 2003;44:5151–5162.
3. Libby RT, Anderson MG, Pang IH, et al. Inherited glaucoma in DBA/2J mice: pertinent disease features for studying the neurodegeneration. *Vis Neurosci.* 2005;22:637–648.
4. Schlamp CL, Li Y, Dietz JA, Janssen KT, Nickells RW. Progressive ganglion cell loss and optic nerve degeneration in DBA/2J mice is variable and asymmetric. *BMC Neuroscience.* 2006;7:66–79.
5. Steele MR, Inman DM, Calkins DJ, Horner PJ, Vetter ML. Microarray analysis of retinal gene expression in the DBA/2J model of glaucoma. *Invest Ophthalmol Vis Sci.* 2006;47:977–985.
6. Soto I, Oglesby E, Buckingham BP, et al. Retinal ganglion cells downregulate gene expression and lose their axons within the optic nerve head in a mouse glaucoma model. *J Neurosci.* 2008; 28:548–561.

7. Bosco A, Inman DM, Steele MR, et al. Reduced retina microglial activation and improved optic nerve integrity with minocycline treatment in the DBA/2J mouse model of glaucoma. *Invest Ophthalmol Vis Sci.* 2008;49:1437–1446.
8. Son JL, Soto I, Oglesby E, et al. Glaucomatous optic nerve injury involves early astrocyte reactivity and late oligodendrocyte loss. *Glia.* 2010;58:780–789.
9. Anderson MG, Smith RS, Hawes NL, et al. Mutations in genes encoding melanosomal proteins cause pigmentary glaucoma in DBA/2J mice. *Nat Genet.* 2002;30:81–85.
10. Howell GR, Libby RT, Marchant JK, et al. Absence of glaucoma in DBA/2J mice homozygous for wild-type versions of Gpnmb and Tyrp1. *BMC Genet.* 2007;8:45.
11. Anderson MG, Libby RT, Mao M, et al. Genetic context determines susceptibility to intraocular pressure elevation in a mouse pigmentary glaucoma. *BMC Biol.* 2006;4:20.
12. Inman DM, Sappington RM, Horner PJ, Calkins DJ. Quantitative correlation of optic nerve pathology with ocular pressure and corneal thickness in the DBA/2 mouse model of glaucoma. *Invest Ophthalmol Vis Sci.* 2006;47:986–996.
13. Niyadurupola N, Broadway DC. Pigment dispersion syndrome and pigmentary glaucoma: a major review. *Clin Exp Ophthalmol.* 2008;36:868–882.
14. Prusky GT, Alam NM, Beekman S, Douglas RM. Rapid quantification of adult and developing mouse spatial vision using a virtual optomotor system. *Invest Ophthalmol Vis Sci.* 2004;45:4611–4616.
15. Douglas RM, Alam NM, Silver BD, McGill TJ, Tschetter WW, Prusky GT. Independent visual threshold measurements in the two eyes of freely moving rats and mice using a virtual-reality optokinetic system. *Vis Neurosci.* 2005;22:677–684.
16. Schmucker C, Seeliger M, Humphries P, Biel M, Schaeffel F. Grating acuity at different luminances in wild-type mice and in mice lacking rod or cone function. *Invest Ophthalmol Vis Sci.* 2005;46:398–407.
17. Pinto LH, Vitaterna MH, Shimomura K, et al. Generation, characterization, and molecular cloning of the Noerg-1 mutation of rhodopsin in the mouse. *Vis Neurosci.* 2005;22:619–629.
18. Pinto LH, Vitaterna MH, Shimomura K, et al. Generation, identification and functional characterization of the nob4 mutation of Grm6 in the mouse. *Vis Neurosci.* 2007;24:111–123.
19. Thomas BB, Shi D, Khine K, Kim LA, Sadda SR. Modulatory influence of stimulus parameters on optokinetic head-tracking response. *Neurosci Lett.* 2010;479:92–96.
20. Cachafeiro M, Bemelmans AP, Canola K, et al. Remaining rod activity mediates visual behavior in adult Rpe65$^{-/-}$ mice. *Invest Ophthalmol Vis Sci.* 2010;1:6835–6842.
21. Boye SE, Boye SL, Pang J, et al. Functional and behavioral restoration of vision by gene therapy in the guanylate cyclase-1 (GC1) knockout mouse. *PLoS One.* 2010;5:e11306.
22. Franco LM, Zulliger R, Wolf-Schnurrbusch UE, et al. Decreased visual function after patchy loss of retinal pigment epithelium induced by low-dose sodium iodate. *Invest Ophthalmol Vis Sci.* 2009;50:4004–4010.
23. Redfern WS, Storey S, Tse K, et al. Evaluation of a convenient method of assessing rodent visual function in safety pharmacology studies: effects of sodium iodate on visual acuity and retinal morphology in albino and pigmented rats and mice. *J Pharmacol Toxicol Methods.* 2011;63:102–114.
24. Porciatti V, Nagaraju M. Head-up tilt lowers IOP and improves RGC dysfunction in glaucomatous DBA/2J mice. *Exp Eye Res.* 2010;90:452–460.
25. Križaj D, Huang W, Furukawa T, Punzo C, Xing W. Plasticity of TRPM1 expression and localization in the wild type and degenerating mouse retina. *Vision Res.* 2010;50:2460–2465.
26. Ryskamp D, Witkovsky P, Barabas P, et al. The polymodal ion channel transient receptor potential vanilloid 4 modulates calcium flux, spiking rate, and apoptosis of mouse retinal ganglion cells. *J Neurosci.* 2011;31;7089–7101.
27. Koehler CL, Akimov NP, Renteria RC. Receptive field center size decreases and firing properties mature in ON and OFF retinal ganglion cells after eye opening in the mouse. *J Neurophysiol.* Published online May 25, 2011.
28. Brainard DH. The Psychophysics Toolbox. *Spat Vis.* 1997;10:433–436.
29. Pelli DG. The VideoToolbox software for visual psychophysics: transforming numbers into movies. *Spat Vis.* 1997;10:437–442.
30. Kleiner M, Brainard D, Pelli D. What's new in Psychtoolbox-3? ECVP Abstract Supplement. *Perception.* 2007;36.
31. Xu HP, Chen H, Ding Q, et al. The immune protein CD3zeta is required for normal development of neural circuits in the retina. *Neuron.* 2010;65:503–515.
32. Kerschensteiner D, Liu H, Cheng CW, et al. Genetic control of circuit function: Vsx1 and Irx5 transcription factors regulate contrast adaptation in the mouse retina. *J Neurosci.* 2008;28:2342–2352.
33. Giolli RA, Blanks RH, Lui F. The accessory optic system: basic organization with an update on connectivity, neurochemistry, and function. *Prog Brain Res.* 2006;151:407–440.
34. Yonehara K, Shintani T, Suzuki R, et al. Expression of SPIG1 reveals development of a retinal ganglion cell subtype projecting to the medial terminal nucleus in the mouse. *PLoS One.* 2008;3:e1533.
35. Zhou X, Li F, Kong L, Chodosh J, Cao W. Anti-inflammatory effect of pigment epithelium-derived factor in DBA/2J mice. *Mol Vis.* 2009;15:438–450.
36. Rangarajan KV, Lawhn-Heath C, Feng L, Kim TS, Cang J, Liu X. Detection of visual deficits in aging DBA/2J mice by two behavioral assays. *Curr Eye Res.* 2011;38:481–491.
37. Burroughs SL, Kaja S, Koulen P. Quantification of deficits in spatial visual function of mouse models for glaucoma. *Invest Ophthalmol Vis Sci*. 2011;52:3654–3659.
38. Puk O, Dalke C, Hrabé de Angelis M, Graw J. Variation of the response to the optokinetic drum among various strains of mice. *Front Biosci.* 2008;13:6269–6275.
39. Zhang X, Zhang M, Avila MY, Ge J, Laties AM. Time course of age-dependent changes in intraocular pressure and retinal ganglion cell death in DBA/2J mouse. *Yan Ke Xue Bao.* 2006;22:184–189.
40. Cahill H, Nathans J. The optokinetic reflex as a tool for quantitative analyses of nervous system function in mice: application to genetic and drug-induced variation. *PLoS One.* 2008;3:e2055.
41. Balkema GW, Mangini NJ, Pinto LH, Vanable JW Jr. Visually evoked eye movements in mouse mutants and inbred strains: a screening report. *Invest Ophthalmol Vis Sci.* 1984;25:795–800.
42. Wong AA, Brown RE. Age-related changes in visual acuity, learning and memory in C57BL/6J and DBA/2J mice. *Neurobiol Aging.* 2007;28:1577–1593.
43. Porciatti V, Chou TH, Feuer WJ. C57BL/6J, DBA/2J, and DBA/2JGpnmb mice have different visual signal processing in the inner retina. *Mol Vis.* 2010;16:2939–2947.
44. Nagaraju M, Saleh M, Porciatti V. IOP-dependent retinal ganglion cell dysfunction in glaucomatous DBA/2J mice. *Invest Ophthalmol Vis Sci.* 2007;48:4573–4579.
45. Saleh M, Nagaraju M, Porciatti V. Longitudinal evaluation of retinal ganglion cell function and IOP in the DBA/2J mouse model of glaucoma. *Invest Ophthalmol Vis Sci.* 2007;48:4564–4572.
46. Nadler JJ, Zou F, Huang H, et al. Large-scale gene expression differences across brain regions and inbred strains correlate with a behavioral phenotype. *Genetics.* 2006;174:1229–1236.
47. Hayhow WR, Webb C, Jervie A. The accessory optic fiber system in the rat. *J Comp Neurol.* 1960;115:187–215.
48. Simpson JI. The accessory optic system. *Annu Rev Neurosci.* 1984;7:13–41.
49. Chesler EJ, Lu L, Shou S, et al. Complex trait analysis of gene expression uncovers polygenic and pleiotropic networks that modulate nervous system function. *Nat Genet.* 2005;37:233–242.
50. Singh SM, Treadwell J, Kleiber ML, Harrison M, Uddin RK. Analysis of behavior using genetical genomics in mice as a model: from alcohol preferences to gene expression differences. *Genome.* 2007;50:877–897.